

Intermittent Phenomena in Switched Systems With High Coupling Strengths

Qingfei Chen, Yiguang Hong, *Senior Member, IEEE*, Guanrong Chen, *Fellow, IEEE*, and David J. Hill, *Fellow, IEEE*

Abstract—In this paper, one kind of intermittency generated by a discontinuous system is studied. Although this system, which is composed of two switched subsystems coupled with a high strength, is nonsmooth, the mechanism of this kind of intermittency can be analyzed with several explicit relations between the intermittency characteristics and the system control parameters. In particular, estimates of “steady-state” values of the system (in the laminar phases) and a critical value for this intermittency can be derived, which are helpful in relevant control systems design. Moreover, some power laws for the observed intermittency are obtained and discussed.

Index Terms—Discontinuous system, intermittency, power law, transverse stability.

I. INTRODUCTION

COMPLEX dynamical phenomena, which are very common among different disciplines, have drawn increasing attention from different research communities over the last few decades. Intermittency, consisting of laminar phases and burst phases, is one of the ubiquitous complex phenomena. In the laminar phase, the system orbits appear to be relatively regular, while in the burst phase the motion of the considered system is quite “violent” and “irregular.” Three simple types of intermittent phenomena (Types I, II, and III) related to three kinds of bifurcations in lower dimensional maps were first identified by Pomeau and Manneville [23]. Then, on–off intermittency, which is related to the transverse instability of (chaotic) attractors confined to a lower dimensional manifold, was systematically explored in [13], [21], and [22]. Because of the low dimension of the manifold, every intermittency exhibits clear and distinct “regular” laminar phases and “irregular” burst phases. Moreover, crisis-induced intermittency was also observed and investigated [20].

New intermittent phenomena similar to on–off intermittency have been observed in recent years. For instance, “icicle” in-

termittency was generated in a rotating system [4]; an interesting intermittency generated by four coupled phase-locked loops (PLLs) was studied thoroughly in [12]; and a new type of intermittency was obtained for two-dimensional (2-D) Hamiltonian systems in the case of large noise strengths [29]. All of these intermittencies appear to fall into the category of (generalized) in–out intermittency as pointed out in [1], [29]. In–out intermittency, as a generalized form of the on–off intermittency, was recently discovered and discussed [1], [2], [25]. It is also associated with some invariant sets in a lower dimensional manifold, but these invariant sets need not be (minimal) chaotic attractors as in the on–off intermittency case. In in–out intermittency, system orbits jump out occasionally from the relatively steady laminar phase to the irregular burst phase and then quickly return to the laminar phase. Consequently, the system trajectory will “blow out” from the lower dimensional subspace in a random-like fashion due to the transverse instability.

In addition to physical systems, intermittency studies can also be applied to other (simple or complex) systems. For example, a relatively simple intermittent phenomenon in a piecewise-linear circuit, associated with a saddle-node bifurcation, was studied in [10]. Both type-I and type-II intermittencies in circuits were investigated in [3] and [14]. Moreover, intermittency has been found to be a useful concept not only in the analysis and control of complex phenomena in bio-systems, in relation to such problems as balancing mechanism, neuronal spike trains, and visual information process [5], [18], [24], but also in applications such as optimization [16] and control of intermittency [19].

More intermittency-related studies are still needed. On the one hand, discovery and classification of new intermittencies are to be carried out, and their underlying generation mechanism and the relationships between different intermittencies are to be investigated. Generally speaking, it is very hard to obtain explicit relations between intermittent characteristics (i.e., the mechanism) and system parameters, though these explicit relations may be very important in systems analysis and design. Moreover, although many intermittent phenomena were generated by smooth or nonsmooth continuous dynamical systems, the study of the intermittency generated by continuous-time discontinuous systems, which are expressed in groups of differential equations with discontinuous right-hand sides, is quite underdeveloped, partially because of the lack of effective tools in nonsmooth analysis and the complexity of many related technical issues [11], [15]. On the other hand, “engineering” approaches, differing from conventional physical methods, focus more on the construction of simply structured systems or the control mechanisms for various complex phenomena, targeting

Manuscript received August 9, 2005; revised May 7, 2006. This work was supported by the National Natural Science Foundation of China under Grant 60425307, Grant 50595411, Grant 10472129, and Grant 60221301. This paper was recommended by Associate Editor C. T. Lin.

Q. Chen is with the Department of Electrical Engineering, Arizona State University, Tempe, AZ 85287 USA (e-mail: qingfei.chen@asu.edu).

Y. Hong is with the Institute of Systems Science, Chinese Academy of Sciences, Beijing 10080, China (e-mail: yghong@iss.ac.cn).

G. Chen is with the Department of Electronic Engineering, City University of Hong Kong, Hong Kong (e-mail: gchen@ee.cityu.edu.hk).

D. J. Hill is with the Department of Information Engineering, Australian National University, Canberra ACT 0200, Australia (e-mail: david.hill@anu.edu.au).

Digital Object Identifier 10.1109/TCSI.2006.883867

practical applications (including intermittency control and generation). These engineering viewpoints may help us better understand the underlying mechanism of intermittent phenomena in an active way and may also suggest new application opportunities, for example, to optimize practical engineering systems or to produce desired dynamical behaviors towards their potential applications (for example, in neurological systems, complex spike codings and patterns may be realized by circuits).

With the rapid and continuous growth of scientific knowledge on nonlinearity and complexity, one tends to take advantage of them rather than removing them as was done in the past. The motivation of our research is to show the intermittency generated by discontinuous systems with simple mechanisms and to provide related analysis methods for potential intermittency design. This study is also expected to show that engineering approaches to analyzing complex dynamical phenomena could provide new ways for better understanding of system behaviors. The main results are summarized here.

- New intermittent phenomena generated by discontinuous dynamics are investigated. More precisely, the mechanism for generating intermittency from a strongly coupled discontinuous system is studied. It is found that intermittency can be easily generated from two identical switched subsystems with a high coupling strength, along a lower dimensional manifold constructed by switching structures, similar to the sliding surface in sliding mode control [28].
- It is hard but important to obtain explicit relations between intermittent characteristics and system parameters, especially from engineering viewpoints. In our study, an approach is developed by taking advantage of the simple structure of the considered nonsmooth dynamics. A critical value of a system parameter (that is, γ), in relation to the occurrence of intermittency, is obtained as an explicit function of system parameters. Moreover, a formula revealing the relation between laminar state values and system parameters is also derived. These explicit relations show how one can change some intermittent behaviors by simply adjusting system parameters.
- With the analysis of the transverse stability for two limit cycles (that is, \mathcal{A} and \mathcal{M}) in a lower dimensional manifold, the observed intermittency is believed to be related to the in–out intermittency, which is a generalized form of the on–off intermittency [1], [25], though the existing results for in–out intermittency were not obtained for discontinuous systems. Moreover, several power laws for intermittency are confirmed. In addition, the low sensitivity to noise of this intermittency is also shown.

The remainder of this paper is organized as follows. In Section II, a new “in–out” intermittency generated by a discontinuous system with coupling and switching is first introduced. Then, in Section III, the dynamics near the onset of this intermittency are analyzed. Furthermore, a critical value for this intermittency and a “steady-state” laminar value are estimated to capture the intermittency characteristics. Following that, in Section IV, statistical analysis of power laws is provided. Finally, some concluding remarks are given in Section V.

II. DISCONTINUOUS DYNAMICS AND INTERMITTENCY

Discontinuous dynamics can effectively yield many interesting dynamical phenomena. For example, one may have already witnessed the significant achievement of control and generation of various chaotic behaviors in different fields. Some effective design methods have been developed by building chaotic systems with simple nonsmooth switching structures [7]–[9], [17], [26].

In this section, a six-dimensional discontinuous system for intermittency generation is introduced. This system is composed of two identical switched subsystems with high coupling strengths. More precisely, consider a system with state vectors $X_i = (x_i, y_i, z_i)^T$, $i = 1, 2$, respectively, as follows:

$$\begin{cases} \dot{X}_1 = f(X_1) + G(X_2 - X_1), & X_1 \in R^3 \\ \dot{X}_2 = f(X_2) + G(X_1 - X_2), & X_2 \in R^3 \end{cases} \quad (1)$$

where the vector fields are

$$f(X_i) = \begin{cases} \begin{pmatrix} a & 1 & 0 \\ -1 & a & 0 \\ 0 & 0 & -2.5 \end{pmatrix} X_i, & \text{if } p(\sqrt{x_i^2 + y_i^2} - q) + z_i \leq 0 \\ \begin{pmatrix} -b & 1 & 0 \\ -1 & -b & 0 \\ 0 & 0 & -2.5 \end{pmatrix} X_i + \begin{pmatrix} 0 \\ 0 \\ 20(a+b) \end{pmatrix}, & \text{if } p(\sqrt{x_i^2 + y_i^2} - q) + z_i > 0 \end{cases} \quad (2)$$

and the coupling matrix is

$$G = \begin{cases} -\rho \begin{pmatrix} 2 & 0 & 0 \\ 0 & 2 & 0 \\ 0 & 0 & 3 \end{pmatrix}, & \text{if } p(\sqrt{x_i^2 + y_i^2} - q) + z_i \leq 0 \\ \rho\gamma \begin{pmatrix} 2 & 0 & 0 \\ 0 & 2 & 0 \\ 0 & 0 & 3 \end{pmatrix}, & \text{if } p(\sqrt{x_i^2 + y_i^2} - q) + z_i > 0 \end{cases} \quad (3)$$

where a, b, ρ, γ, p , and q are (control) parameters satisfying

$$p > 0; \quad q > 0; \quad 1 > \gamma > 0, \quad \rho > \frac{1}{1-\gamma} \gg a > b > 0. \quad (4)$$

Note that the coupling feedback gain ρ is set to be much larger than the parameters a and b in this nonsmooth system. In other words, system (1) is a strongly coupled system.

System (1) has two simple subsystems with switching structures, and its coupling control terms dominate the dynamical behavior most of the time (since $\rho \gg a > b$). In the last two decades, control with switching surfaces has been widely used in the generation of various chaotic attractors; the switching surfaces used in this paper are similar to those used in some chaos generation control (like the one used in [17]). Here, it is worthwhile to point out that the dominant coupling terms play a key role in the intermittent behaviors of system (1); they force the system states to repeatedly move near the switching surfaces, evoking blowouts unpredictably.

For each subsystem, there are two regions, denoted by

$$\begin{cases} C_i^1 = \left\{ (x_i, y_i, z_i) \mid p(\sqrt{x_i^2 + y_i^2} - q) + z_i \leq 0 \right\} \\ C_i^2 = \left\{ (x_i, y_i, z_i) \mid p(\sqrt{x_i^2 + y_i^2} - q) + z_i > 0 \right\} \end{cases} \quad (5)$$

for $i = 1, 2$, which are separated by two switching surfaces

$$S_i = \left\{ (x_i, y_i, z_i) \left| p \left(\sqrt{x_i^2 + y_i^2} - q \right) + z_i = 0 \right. \right\}, \quad i = 1, 2.$$

Hence, the dynamics of system (1) occur in a six-dimensional (6-D) space, which is made up of four nonoverlapping regions and partitioned by two switching hyper-surfaces in R^6

$$\bar{S}_i = \left\{ (x_1, y_1, z_1, x_2, y_2, z_2) \left| p \left(\sqrt{x_i^2 + y_i^2} - q \right) + z_i = 0 \right. \right\}, \quad i = 1, 2.$$

Set

$$\begin{aligned} R_i &= \sqrt{x_i^2 + y_i^2} \\ \theta_i &= \arctan \left(\frac{y_i}{x_i} \right), \quad i = 1, 2. \end{aligned}$$

Then, (R_1, θ_1) and (R_2, θ_2) are the polar coordinates for (x_1, y_1) and (x_2, y_2) , respectively, and $x_i = R_i \cos(\theta_i)$, $y_i = R_i \sin(\theta_i)$. Based on this, system (1) can be rewritten as follows.

- If $p(R_i - q) + z_i \leq 0$, then

$$\begin{cases} \dot{R}_i = aR_i - 2\rho\Gamma_i \\ \dot{z}_i = -2.5z_i - 3\rho(z_j - z_i), \quad i \neq j \\ \dot{\theta}_i = -2 - 2\rho \frac{x_i y_j - x_j y_i}{R_i^2}, \quad i \neq j \end{cases} \quad (6)$$

where

$$\Gamma_i = \frac{x_i x_j + y_i y_j - R_i^2}{R_i}, \quad i \neq j, i, j = 1, 2. \quad (7)$$

It is easy to see that $\Gamma_1 + \Gamma_2 \leq 0$, where equality holds if and only if $x_1 = x_2, y_1 = y_2$.

- If $p(R_i - q) + z_i > 0$, then

$$\begin{cases} \dot{R}_i = -bR_i + 2\rho\Gamma_i \\ \dot{z}_i = -2.5z_i + 20(a+b) + 3\rho\gamma(z_j - z_i), \quad j \neq i \\ \dot{\theta}_i = -2 + 2\rho\gamma \frac{x_i y_j - x_j y_i}{R_i^2}, \quad j \neq i. \end{cases} \quad (8)$$

In the intermittency analysis, laminar and burst magnitudes (measured by R_i and $z_i, i = 1, 2$) are very useful. The equations in R_i and $z_i, i = 1, 2$, will be considered in more detail below.

Set the system parameters as

$$\begin{cases} a = 0.03 \\ b = 0.01 \\ \rho = 2 \\ p = 1 \\ q = 20 \\ \gamma = 0.34. \end{cases} \quad (9)$$

$$(10)$$

In all of the numeral simulations of this paper, we adopt the Runge–Kutta method with step size 10^{-3} .

Figs. 1 and 2 show the intermittent behaviors of system (1): the trajectories of $z_1(t)$ and $z_2(t)$ occasionally burst, thus we refer to them as the burst state. After that, the trajectories settle

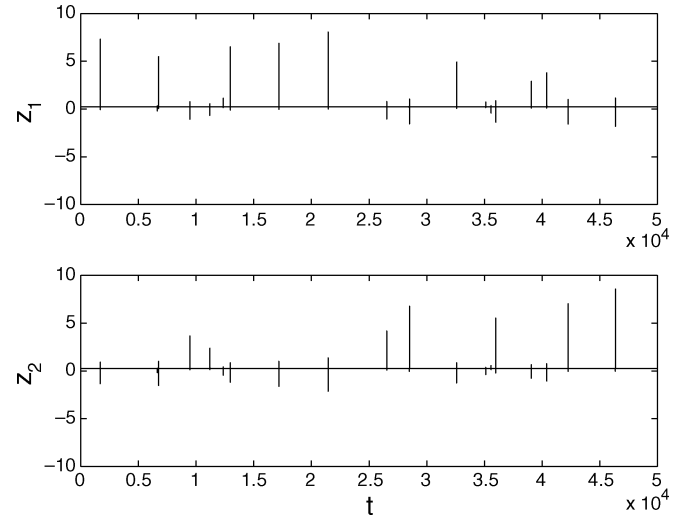


Fig. 1. $z_i; (i = 1, 2)$ of system (1).

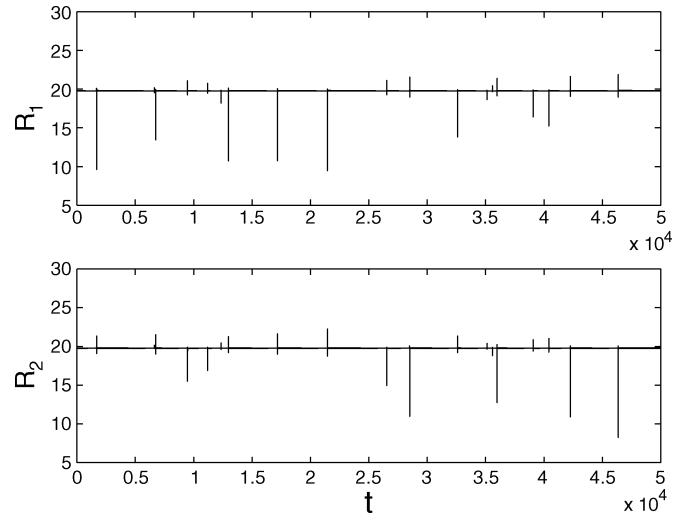


Fig. 2. $R_i (i = 1, 2)$ of system (1).

down and stay in this steady state for a relatively long time, which is referred to as the laminar state. Clearly, z_1 and z_2 show burst/laminar phases simultaneously.

Both z_i and $R_i = \sqrt{x_i^2 + y_i^2} (i = 1, 2)$ demonstrate an intermittency pattern, where $z_i (i = 1, 2)$ and $R_i (i = 1, 2)$ of system (1) are almost synchronized, respectively, moving around constant real numbers in all laminar phases. These constant numbers (denoted by z_* and R_* , respectively) will be determined in the next section. Moreover, Fig. 2 shows that the intermittency of $R_i(t) (i = 1, 2)$ shares the same timing of that for $z_i (i = 1, 2)$. In fact, $x_1(t) - x_2(t)$ and $y_1(t) - y_2(t)$ also evolve “intermittently” in sawtooth waves, which will also be shown and explained in Section III.

In the laminar phase, the system orbit goes across the switching surface $S_i (i = 1, 2)$ back and forth almost all of the time because of the dominant coupling terms in the same way as occurs in the familiar sliding mode control, where the controlled system keeps switching back and forth along its sliding surface [28].

III. INTERMITTENCY ANALYSIS

Because of the complexity of intermittency, numerical analysis is widely used for study. It is not easy to formulate simple yet meaningful relations between its characteristics and system parameters. Nevertheless, we attempt to analyze the underlying mechanism of the intermittency generated by the discontinuous system (1), deriving some explicit characteristics such as the critical value of this intermittency and the “steady-state” values (in laminar phases). These results will help better understand how this intermittency is generated and how its associated dynamical behaviors can be modified by adjusting control parameters.

As mentioned above, previous works on intermittency were mainly concerned with its dynamical behavior near the onset of the intermittency, that is, a burst will appear when a specific parameter is (slightly) changed around the critical value of the intermittency. Here, for system (1), we focus on the control parameter γ and denote its critical value by γ_c . More precisely, we focus on the system dynamics around this critical value, particularly the following two cases.

- 1) For γ values near γ_c with $\gamma < \gamma_c$, $z_i(t)$ and $R_i(t)$ ($i = 1, 2$) are synchronized.
- 2) For γ values near γ_c with $\gamma > \gamma_c$, intermittency of $z_i(t)$ and $R_i(t)$ ($i = 1, 2$) occurs.

A. Critical Value for Intermittency

There is a certain critical value of a control parameter (γ here) related to intermittency, though its explicit expression is difficult to derive in general. Although there are few effective methods for dealing with discontinuous dynamics, based on the special structure of the nonsmooth system (1), one can estimate the critical value γ_c in a simple way.

Let us focus on the switching surfaces, since the dynamics move around them most of the time. As mentioned, in the whole space there are four regions divided by the switching surfaces \bar{S}_i , $i = 1, 2$, given as follows:

$$\begin{cases} \Sigma_1 : \{ (X_1^T, X_2^T) \in \mathbf{R}^6 \mid X_1 \in C_1^1, X_2 \in C_2^1 \} \\ \Sigma_2 : \{ (X_1^T, X_2^T) \in \mathbf{R}^6 \mid X_1 \in C_1^1, X_2 \in C_2^2 \} \\ \Sigma_3 : \{ (X_1^T, X_2^T) \in \mathbf{R}^6 \mid X_1 \in C_1^2, X_2 \in C_2^1 \} \\ \Sigma_4 : \{ (X_1^T, X_2^T) \in \mathbf{R}^6 \mid X_1 \in C_1^2, X_2 \in C_2^2 \} \end{cases} \quad (11)$$

where C_i^1 and C_i^2 were defined in (5).

From numerical simulations, we observe that, when both subsystems are in the steady state (or in the laminar phase of the on–off intermittent phenomenon), the system orbit actually goes through the switching surfaces S_i ($i = 1, 2$) and the four regions Σ_j , $j = 1, 2, 3, 4$, frequently in the following sequences: $\Sigma_1 \rightarrow \Sigma_2 \rightarrow \Sigma_4 \rightarrow \Sigma_3 \rightarrow \Sigma_1 \rightarrow \dots$, or symmetrically, $\Sigma_1 \rightarrow \Sigma_3 \rightarrow \Sigma_4 \rightarrow \Sigma_2 \rightarrow \Sigma_1 \rightarrow \dots$. Because the two subsystems are identical, we only take one of the two sequences to analyze.

Denote these short duration lengths in regions $\Sigma_1, \Sigma_2, \Sigma_3$, and Σ_4 by t_{11}, t_{12}, t_{21} , and t_{22} , respectively. Since the two subsystems are identical, we assume $t_{12} = t_{21} = t_0$.

Recalling (6) and (8) and noticing $x_1x_2 + y_1y_2 = R_1R_2 \cos(\theta_1 - \theta_2)$, we have

$$\begin{cases} \dot{R}_i = (a + 2\rho)R_i - 2\rho \cos(\theta_1 - \theta_2)R_j, \\ \quad \text{if } p(R_i - q) + z_i < 0 \\ \dot{R}_i = -(b + 2\rho\gamma)R_i + 2\rho\gamma \cos(\theta_1 - \theta_2)R_j, \\ \quad \text{otherwise} \end{cases} \quad i \neq j. \quad (12)$$

Since the two subsystems are identical, $R_1 \approx R_2$ in the steady state. Therefore, after one round of motion with $T = t_{11} + t_{12} + t_{21} + t_{22}$, the increment of R_i ($i = 1, 2$) in this steady state will approximate 0, i.e.,

$$\begin{aligned} & [(a + 2\rho) - 2\rho \cos(\theta_1 - \theta_2)] R_1(t_{11} + t_{12}) + \\ & [-(b + 2\rho\gamma) + 2\rho\gamma \cos(\theta_1 - \theta_2)] R_1(t_{22} + t_{21}) \approx 0 \end{aligned}$$

which implies that

$$\frac{t_{11} + t_0}{t_0 + t_{22}} \approx \frac{b + 2\rho\gamma(1 - \cos(\theta_1 - \theta_2))}{a + 2\rho(1 - \cos(\theta_1 - \theta_2))} = \gamma'. \quad (13)$$

Thus

$$t_0 \approx \frac{\gamma' t_{22} - t_{11}}{1 - \gamma'}. \quad (14)$$

Set $d = \sqrt{(x_1 - x_2)^2 + (y_1 - y_2)^2}$. Then, in the four different regions, we have:

- in Σ_1 , $\dot{d} = (a + 4\rho)d := d_1$;
- in Σ_2 , $\dot{d} = (2\rho - 2\rho\gamma)d + ((ax_1 + bx_2)(x_1 - x_2) + (ay_1 + by_2)(y_1 - y_2))/d := d_2$;
- in Σ_3 , $\dot{d} = (2\rho - 2\rho\gamma)d + ((-bx_1 - ax_2)(x_1 - x_2) + (-by_1 - ay_2)(y_1 - y_2))/d := d_3$;
- in Σ_4 , $\dot{d} = (-b - 4\rho\gamma)d := d_4$.

Consequently, the total increment of d after one round of switching through C_i^j , $i = 1, 2$, $j = 1, 2$, is

$$\begin{aligned} \hat{d} &= d_1 t_{11} + d_2 t_{12} + d_3 t_{21} + d_4 t_{22} \\ &\approx [(a + 4\rho)(t_0 + t_{11}) + (-b - 4\rho\gamma)(t_0 + t_{22})] d. \end{aligned} \quad (15)$$

Combining (14) and (15) gives

$$\hat{d} \approx \frac{t_{22} - t_{11}}{1 - \gamma'} ((a + 4\rho)\gamma' - (b + 4\rho\gamma)) d. \quad (16)$$

Note that

$$T = t_{11} + t_{22} + t_{12} + t_{21} = t_{11} + t_{22} + 2t_0 \approx \frac{1 + \gamma'}{1 - \gamma'} (t_{22} - t_{11}) \quad (17)$$

or equivalently $t_{22} - t_{11} \approx ((1 - \gamma')/(1 + \gamma'))T$. Therefore

$$\hat{d} \approx \frac{T}{1 + \gamma'} ((a + 4\rho)\gamma' - (b + 4\rho\gamma)) d$$

which implies, according to (13), that

$$\hat{d} \approx 2T\rho \frac{(b - a\gamma)(1 + \cos(\theta_1 - \theta_2))}{a + b + 2\rho(1 + \gamma)(1 - \cos(\theta_1 - \theta_2))} d. \quad (18)$$

Next, consider the “steady” state, where d remains almost invariant (or $\hat{d} \approx 0$). To guarantee $\hat{d} = 0$, we have two choices: $\theta_1 - \theta_2 = \pm\pi$ or $b = a\gamma$. Here, we focus on $b = a\gamma$, which shows a critical relation between γ and the change of d (we

TABLE I
CRITICAL VALUE γ_c VERSUS b

b	0.008	0.01	0.012	0.014	0.016	0.018
$\bar{\gamma}_c$	0.2690	0.3351	0.4025	0.4686	0.5385	0.6077
$\frac{b}{a}$	0.2658	0.3333	0.4006	0.4663	0.5337	0.6

will consider the case of $\theta_1 - \theta_2 = \pm\pi$ later in the analysis of dynamical behaviors). Thus, we obtain

$$\gamma_c = \frac{b}{a} \quad (19)$$

which will be further shown later to be quite accurate for the intermittent phenomenon in system (1), specifically in the analysis of the dynamics near $\gamma = \frac{b}{a}$ and power laws.

As in many previous works, we can also numerically obtain an estimated critical value (denoted by $\bar{\gamma}_c$) for γ_c . For comparison, Table I shows that the numerical values are very close to the values calculated by (19).

From (19), it is clear that one can change the critical point easily by adjusting system parameters.

Note that our approach proposed here is mainly based on the observation that system (1) is almost “linear” if there were no switching. In other words, the idea of this approach may be extended to dynamical analysis for the systems consisting of “linear” systems switching among them.

In the next two subsections, we will consider the intermittency by changing the parameter γ in a small neighborhood of b/a . There are two main cases: 1) γ is slightly smaller than b/a and 2) γ is slightly larger than b/a .

B. Case 1): $\gamma < \frac{b}{a}$

We first consider the case that γ is slightly smaller than b/a . In this case, according to (18), $\hat{d} > 0$ if $|\theta_1 - \theta_2| < \pi$. So, d (and relevantly, $|\Gamma_i|$, $i = 1, 2$) increases, and $|x_1 - y_1|$ and $|x_2 - y_2|$ of system (1) keep increasing, though z_1 and z_2 of system (1) become synchronized. Hence, $d = \sqrt{(x_1 - x_2)^2 + (y_1 - y_2)^2}$ will increase until it reaches the maximum value d^{\max} when $\theta_1 - \theta_2$ equals either π or $-\pi$ (namely, $x_1 = -x_2$ and $y_1 = -y_2$). Because the coupling terms $2\rho|\Gamma_i|$ (or $2\rho\gamma|\Gamma_i|$) are much larger than aR_i (or bR_i) $i = 1, 2$, the dynamics of the system are mainly determined by the coupling terms. More specifically:

- if $p(R_i - q) + z_i \leq 0$, then

$$\dot{R}_i = aR_i - 2\rho\Gamma_i \approx -2\rho\Gamma_i > 0$$

because Γ_i , $i = 1, 2$, are negative, which means R_i will increase quickly until the two subsystems reach the switching surfaces S_i , $i = 1, 2$, respectively;

- if $p(R_i - q) + z_i > 0$, then

$$\dot{R}_i = -bR_i + 2\rho\gamma\Gamma_i \approx 2\rho\gamma\Gamma_i < 0$$

which implies that R_i will decrease rapidly until the two subsystems reach S_i , $i = 1, 2$, respectively.

Thus, we can see that the system trajectory converges to the switching surfaces from both sides.

Denote z_* and $R_* = q - (z_*/p)$ as the steady-state values of z_i and R_i ($i = 1, 2$), which will be determined as follows.

Let us revisit (6) and (8) by taking $z_1 = z_2 = z_*$ in the steady state.

- If $p(R_i - q) + z_i \leq 0$, then

$$\begin{cases} \dot{R}_i = aR_i - 2\rho\Gamma_i = (a + 4\rho)R_i \\ \dot{z}_i = -2.5z_i. \end{cases} \quad (20)$$

- If $p(R_i - q) + z_i > 0$, then

$$\begin{cases} \dot{R}_i = -bR_i + 2\rho\gamma\Gamma_i = -(b + 4\rho\gamma)R_i \\ \dot{z}_i = -2.5z_i + 20(a + b). \end{cases} \quad (21)$$

As mentioned in the previous section, the trajectory of subsystem i crosses S_i back and forth, over and over again, with a high frequency because of the high-gain coupling. Thus, the trajectory goes through S_i from C_i^1 to C_i^2 and then come back to C_i^1 again within a very short time period of time. In other words, the moment t_1 when the trajectory crosses S_i from C_i^1 to C_i^2 is almost the same as the moment t_2 when the system goes through S_i from C_i^2 to C_i^1 , that is, $t_2 \cong t_1$. Now, we check the trajectory directions in the two cases in the phase space (R, z) , that is, using (20) and (21), we check the directions defined by

$$v_i^1(t_1) = \left. \frac{\dot{z}_i}{\dot{R}_i} \right|_{t=t_1} = \frac{-2.5z_i(t_1)}{(a + 4\rho)R_i(t_1)} \quad (22)$$

$$v_i^2(t_2) = \left. \frac{\dot{z}_i}{\dot{R}_i} \right|_{t=t_2} = \frac{-2.5z_i(t_2) + 20(a + b)}{-(b + 4\rho\gamma)R_i(t_2)}. \quad (23)$$

By neglecting the tiny difference between t_1 and t_2 (since $t_1 \cong t_2$), it is easy to see that z_i would stay invariant if and only if $v_i^1 = v_i^2$, $i = 1, 2$. Fig. 3 sketches the system orbits in the case of $v_i^1 = v_i^2$. From this observation, we can derive the value of z_* from $v_i^1 = v_i^2$, i.e.,

$$1 = \frac{v_i^1}{v_i^2} = \frac{2.5z_*(b + 4\rho\gamma)}{[-2.5z_* + 20(a + b)](a + 4\rho)}$$

yielding

$$z_* = \frac{8(a + b)(a + 4\rho)}{(a + b) + 4\rho(1 + \gamma)}. \quad (24)$$

This makes the adjustment of the steady-state value easier.

In fact, with the parameter setting given in (9), $4\rho \gg a$ and $4\rho(1 + \gamma) \gg a + b$, and then we can have a “simplified” version of (24):

$$z_* \approx \frac{8(a + b)}{1 + \gamma}. \quad (25)$$

Since the system orbits move along the switching surface, we can obtain the “steady” value R_* as

$$R_* = q - \frac{z_*}{p} = q - \frac{8(a + b)(a + 4\rho)}{p(a + b) + 4\rho p(1 + \gamma)} \quad (26)$$

or simply

$$R_* \approx q - \frac{8(a + b)}{p(1 + \gamma)}. \quad (27)$$

In this case, we also have

$$\Gamma_i = -2R_i = -2R_*, i = 1, 2, \quad d = 2R_*. \quad (28)$$

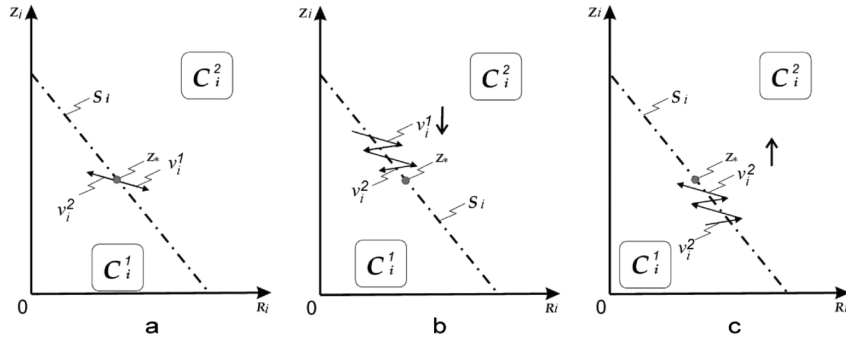


Fig. 3. Motions in the cases of $(v_i^1/v_i^2) = 1$, $(v_i^1/v_i^2) > 1$, and $(v_i^1/v_i^2) < 1$ near $z_i = z_*$, $i = 1, 2$.

Thus, $\frac{v_i^1}{v_i^2} > 1$, which means that the trajectory moves downwards along the switching surface with the value of z_i decreasing back to z_* . A similar analysis can be given for the case of $\Delta < 0$ with $\frac{v_i^1}{v_i^2} < 1$. Fig. 3 shows the system orbits in three cases: $\frac{v_i^1}{v_i^2} = 1$, $\frac{v_i^1}{v_i^2} > 1$, and $\frac{v_i^1}{v_i^2} < 1$. Therefore, on the switching surface $\bar{S}_1 \cap \bar{S}_2$, there is an “attractive” lower dimensional manifold for system (1) as

$$\begin{aligned} \mathcal{H} &= \{(x_1, y_1, z_1, x_2, y_2, z_2) \in \bar{S}_1 \cap \bar{S}_2 | z_i = z_*, i = 1, 2\} \\ &= \{(x_1, y_1, z_1, x_2, y_2, z_2) \in \mathbf{R}^6 | x_i^2 + y_i^2 = R_*^2, \\ &\quad z_i = z_*, i = 1, 2\}. \end{aligned}$$

Moreover, since the system orbits move near the switching surfaces, we can see that z_i near the value z_* tends to become z_* . In fact, if $z_i = z_* + \Delta$ with $\Delta > 0$, then, by (25), we have

$$\begin{aligned} \frac{v_i^1}{v_i^2} &\approx \frac{2.5(z_* + \Delta)(b + 4\rho\gamma)}{[-2.5(z_* + \Delta) + 20(a + b)](a + 4\rho)} \\ &> \frac{-2.5z_*(b + 4\rho\gamma)}{[-2.5z_* + 20(a + b)](a + 4\rho)} = 1. \end{aligned}$$

Furthermore, with $|\theta_1 - \theta_2| \rightarrow \pi$ (due to $d \rightarrow d^{\max}$), an attractor, described by a limit cycle in the form of

$$\mathcal{A} = \{(x_1, y_1, z_1, x_2, y_2, z_2) \in \mathbf{R}^6 | x_1 = -x_2, y_1 = -y_2, x_i^2 + y_i^2 = R_*^2, z_i = z_*, i = 1, 2\} \subset \mathcal{H}$$

is attractive.

With (9), we take

$$\gamma = 0.32 < \frac{b}{a} = \frac{1}{3}. \tag{29}$$

Denote $\langle w \rangle$ as the mean value of any variable w . Numerical results show that the average values of z_i ($i = 1, 2$) are $\langle z_1 \rangle = 0.2424$ and $\langle z_2 \rangle = 0.2424$, which is equal to the theoretical value $z_* = 0.2424$ according to (24) [or (25)]. Note that the derivation of (24) for z_* is based on the assumption that the high-gain coupling terms keep the system moving near the switching surfaces, which may not apply when the value of γ is substantially changed. However, when γ is limited in a moderate range near γ_c , we can see that slight changes of some parameters given in (9) do not influence the value of z_* . Because $z_1(t) \approx z_2(t)$, here we make a comparison between $\frac{z_1 + z_2}{2}$ and z_* . From Table II, one can see that $\langle \frac{z_1 + z_2}{2} \rangle$ keeps close to the value $z_* = 0.2424$ when p and q change in the intervals $p \in [0.4, 1]$ and $q \in$

TABLE II
VALUES OF $\langle (z_1 + z_2) / (2) \rangle$ WHEN $\gamma = 0.32$

$p \setminus q$	14	16	18	20
0.4	0.2424	0.2424	0.2424	0.2424
0.6	0.2404	0.2424	0.2424	0.2424
0.8	0.2424	0.2424	0.2424	0.2424
1	0.2424	0.2424	0.2424	0.2424

[14, 20], respectively. In other words, these numerical simulations are consistent with the analysis given above.

Moreover, the mean values of R_i , $i = 1, 2$, are $\langle R_i \rangle = 19.7846$, roughly equal to $R_* = -z_*/p + q = 19.7576$. $\langle R_1 \rangle = 19.7846$, and $\langle R_2 \rangle = 19.7846$, which shows that the mean values of R_i , $i = 1, 2$. In addition, the numerical results show $\langle \Gamma_1 \rangle = -39.5692$ and $\langle \Gamma_2 \rangle = -39.5692$, which well match the value $\Gamma_i = -2R_* = -39.5152 < 0$ calculated from (28).

Figs. 4 and 5 show the numerical results for the projections of the steady-state trajectory, which basically verify the stability of set \mathcal{A} and the relations $x_1(t) = -x_2(t)$ and $y_1(t) = -y_2(t)$ in the steady state (when $\dot{d} = 0$). Moreover, the value of $d(t)$ increases rapidly from its initial condition to $d = d^{\max} = \sqrt{(x_1 - x_2)^2 + (y_1 - y_2)^2} = 2R_*$. For parameters (9) and $\gamma = 0.32$, $d^{\max} = 2R_* = 39.5152$. Fig. 6 shows the results with $\langle d \rangle = 39.5692 \approx d^{\max}$, which confirms the above analysis.

The dynamics in the set \mathcal{A} is expressed as

$$\dot{X}_i = f(X_i) - 2GAX_i, \quad i = 1, 2 \tag{30}$$

where

$$A = \begin{pmatrix} 1 & 0 & 0 \\ 0 & 1 & 0 \\ 0 & 0 & 0 \end{pmatrix}$$

and $f(X_i)$ and G were defined in (1). Recalling (6) and (8), we have

$$\dot{\theta}_i = -1 \pm 2\rho \frac{x_i y_j - x_j y_i}{R_i^2}.$$

For convenience, denote $\Omega_i = (x_i y_j - x_j y_i) / (R_i^2)$ for $i \neq j$. As $\theta_1 - \theta_2 \rightarrow \pm\pi$, we have $\dot{d} \rightarrow 0$ and $\Omega_i(t) \rightarrow 0$, $i = 1, 2$, which is consistent with the numeral results $\langle \Omega_i \rangle = 0.0003$. Therefore, $\dot{\theta}_i \rightarrow -1$. In other words, the system orbits move (almost) periodically with a period of 2π since $\theta_i(t) = \theta_i(0) - t$.

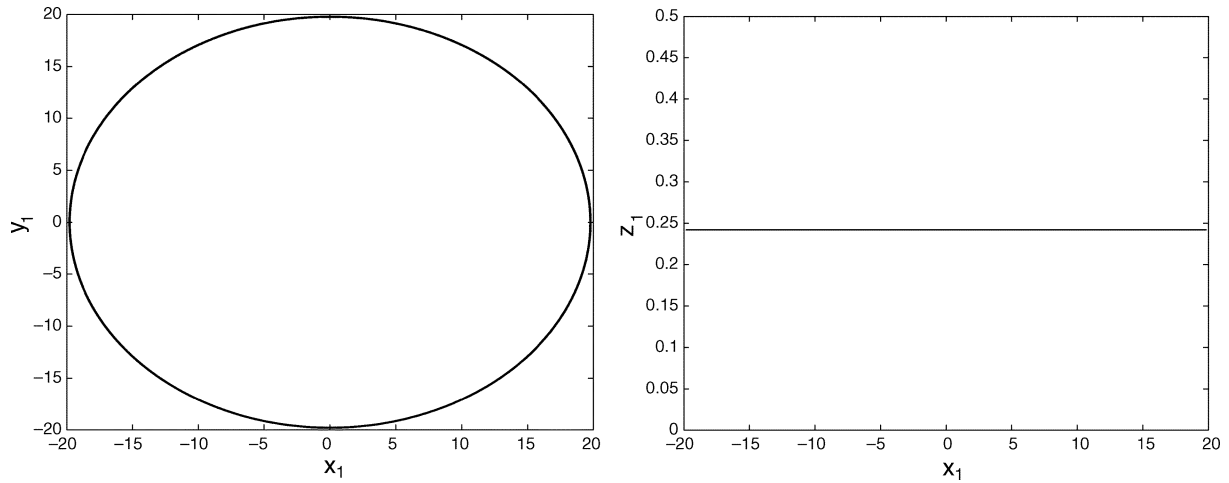


Fig. 4. Two projections of the steady-state trajectory show the limit cycle \mathcal{A} .

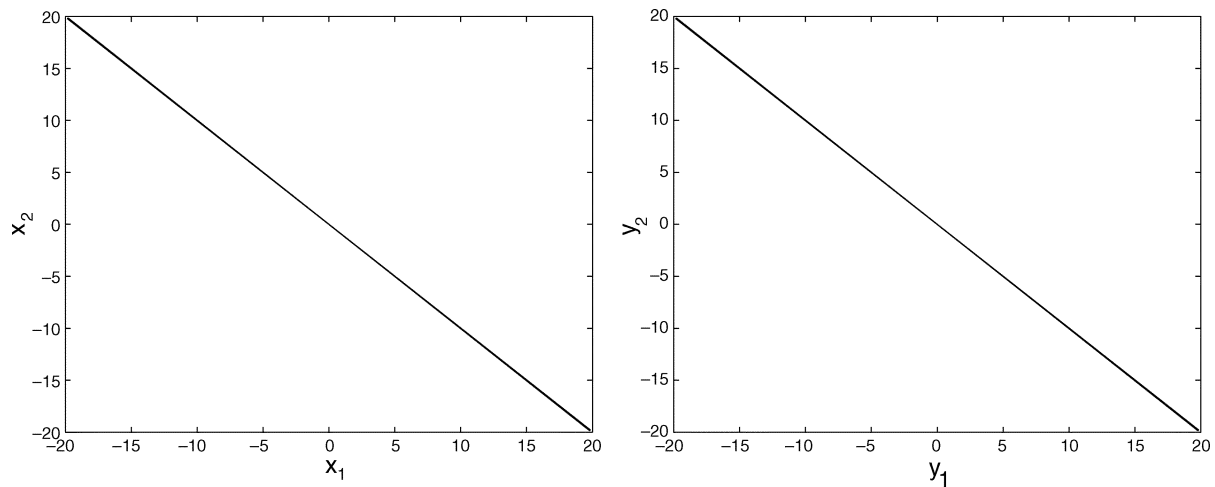


Fig. 5. $x_1(t) \approx -x_2(t)$, $y_1(t) \approx -y_2(t)$ in the steady state.

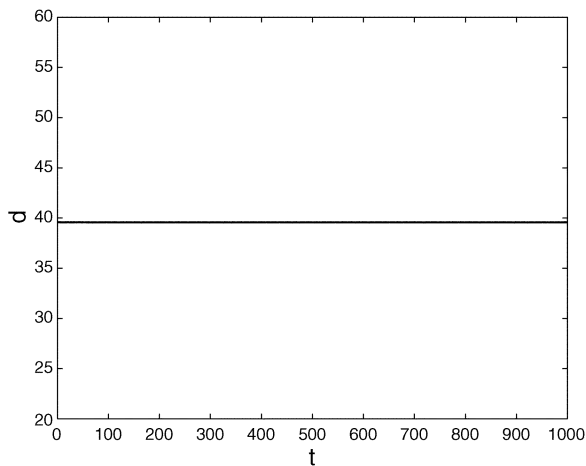


Fig. 6. Trajectory $d(t)$.

Thus, the trajectory generated by (30) with parameters (9) and (29), as verified in Figs. 4 and 5, forms the limit cycle \mathcal{A} .

C. Case 2): $\gamma > \frac{b}{a}$

This subsection studies the intermittency case when γ is slightly larger than b/a . Note that \hat{d} in (18) is a monotonously decreasing function of γ . Therefore, if $\gamma > \frac{b}{a}$, then $\hat{d} < 0$ and d is decreasing and approaching 0 (that is, $d \rightarrow 0$ or, equivalently, $|x_1 - x_2| \rightarrow 0$, $|y_1 - y_2| \rightarrow 0$).

What is the underlying mechanism that governs the transitions between laminar phases and burst phases? In fact, when $d \approx 0$, the two subsystems tend to be completely synchronized. Define a set for the complete synchronization of the two subsystems as

$$\mathcal{M} = \{(x_1, y_1, z_1, x_2, y_2, z_2) \in \mathbf{R}^6 | x_1 = x_2, y_1 = y_2, x_i^2 + y_i^2 = R_*^2, z_i = z_*, i = 1, 2\}$$

where z_* and R_* are obtained from (24) and (26), respectively. Similarly, we also have \mathcal{H} and \mathcal{A} with z_* and R_* based on (24) and (26). Clearly, \mathcal{M} is a limit cycle embedded in the low-dimensional manifold \mathcal{H} .

In fact, \mathcal{M} is attractive in \mathcal{H} due to $d \rightarrow 0$, but it is transversely unstable. In other words, it is an “exit” set of \mathcal{H} and

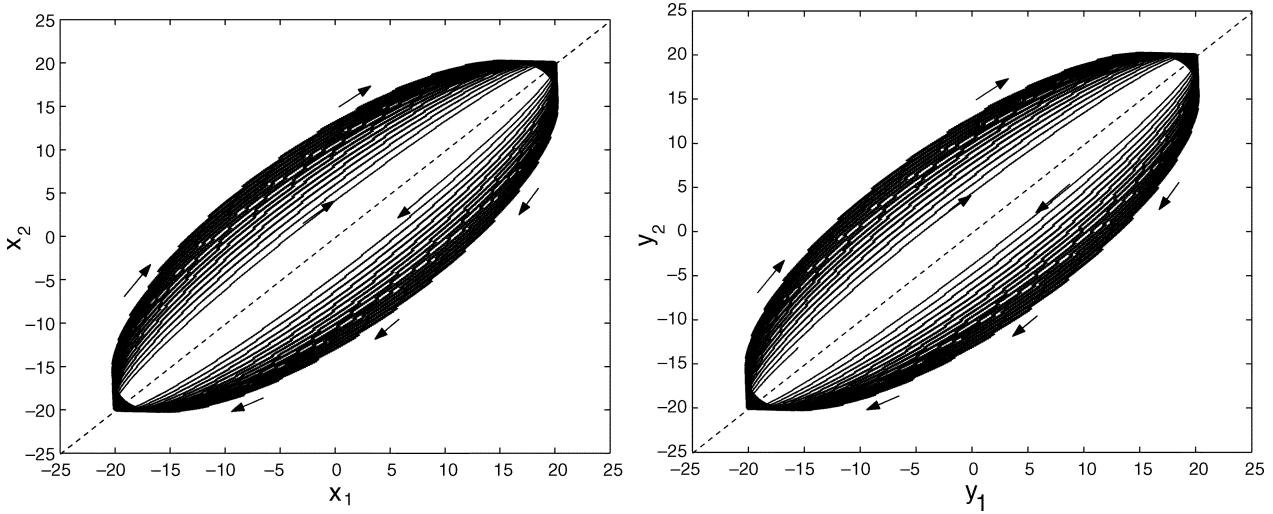


Fig. 7. System orbit moves back to \mathcal{M} .

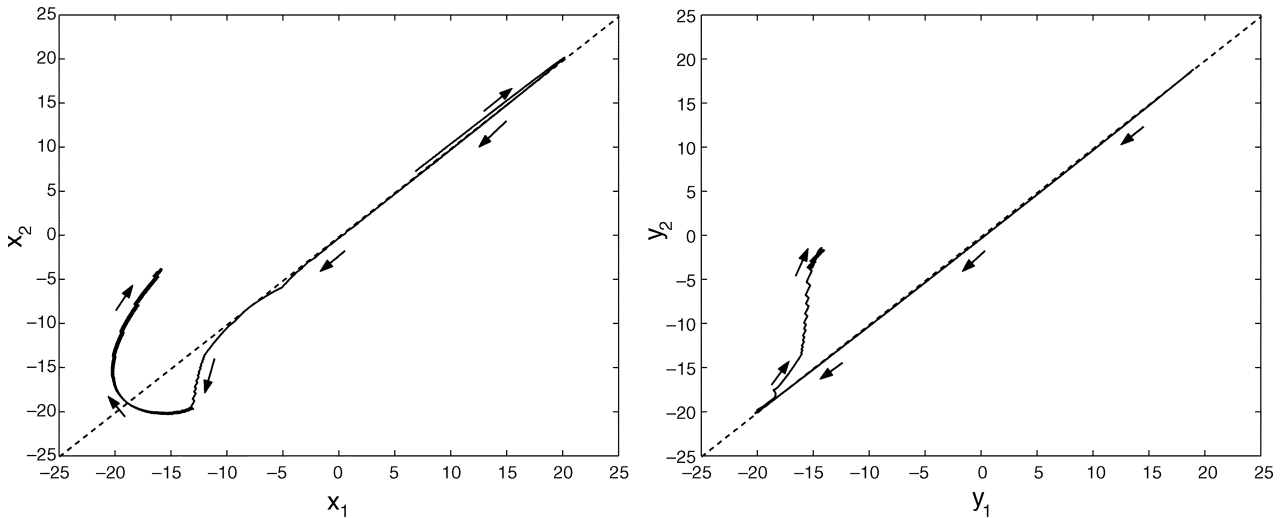


Fig. 8. System orbit approaches \mathcal{M} and jumps out thereafter.

a blowout will occur near \mathcal{M} (sketched by the dashed lines in Figs. 7 and 8). Fig. 8 reveals a jump process from a laminar phase to a burst phase, while Fig. 7 shows the process when the system reenters its laminar phase.

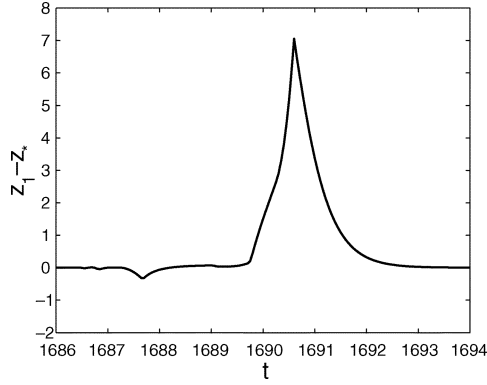
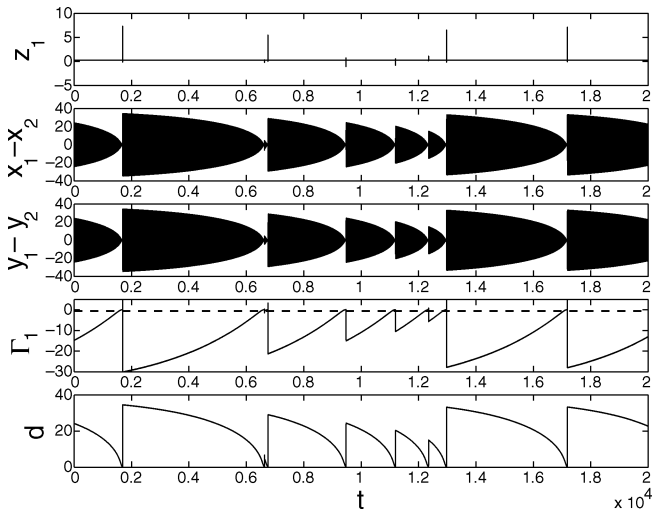
In fact, when d is not very small and the coupling terms $2\rho|\Gamma_i|$ (or $2\rho\gamma|\Gamma_i|$) are much larger than aR_i (or bR_i), $i = 1, 2$, one has $z_i \approx z_*$, $i = 1, 2$ and the system orbit stays quietly to form its laminar phase. However, when d (and correspondingly $\theta_1 - \theta_2$ and $|\Gamma_i|$, $i = 1, 2$) becomes small enough as $d \rightarrow 0$, the coupling terms are too weak to stop the subsystems from moving without switching. The two subsystems tend to be completely synchronized but the system variables burst before the system dynamics exactly reaches \mathcal{M} . Once these state variables jump out, the coupling terms begin dominating the system again and it goes back to the laminar phase of z_i , $i = 1, 2$. Thus, one can expect that the variable d (along with $|x_i - x_j|$, $|y_i - y_j|$, Γ_i) keeps jumping out suddenly and decreasing monotonously in a sawtooth fashion. This analysis can be clearly verified by the numerical results shown in Fig. 10, which demonstrate that $|x_i - x_j|$, $|y_i - y_j|$, $|\Gamma_i|$, and d are all going down (or Γ_i is going

up because it is negative), when z_i , $i = 1, 2$, stay in the laminar phase. The bursts of z_i , $i = 1, 2$, can also be explained. When the system is near \mathcal{M} and X_1 and X_2 are not in the same region or, to be precise, in regions Σ_2 or Σ_3 (without loss of generality, considering the case Σ_3 , that is, $X_1 \in C_1^1$ and $X_2 \in C_2^2$), we have

$$\begin{cases} \dot{z}_1 = -2.5z_1 + 3\rho\gamma(z_2 - z_1) + 20(a + b) \\ \dot{z}_2 = -2.5z_2 - 3\rho(z_1 - z_2). \end{cases}$$

Take $z_0 = z_2 - z_1$. $\dot{z}_0 = 2.5[\rho(1 - \gamma) - 1]z_0 + 20(a + b)$ shows that z_0 diverges very quickly (that is, z_1 and z_2 are clearly desynchronized), which implies that \mathcal{M} is unstable in the \mathcal{H}^\perp -direction (that is, \mathcal{M} is transversely unstable in \mathcal{H}). This is because the coupling strength $\rho(1 - \gamma) > 1$ from (4), and there is no crossover on the switching surfaces during bursting (see Fig. 8).

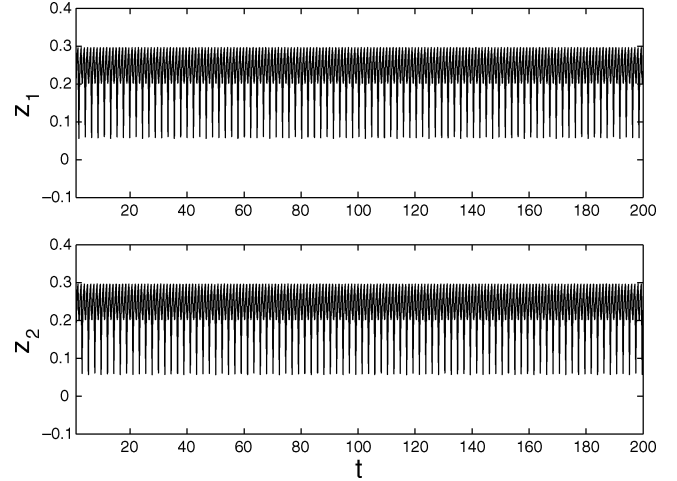
When the coupling terms become dominant (when the system state is away from \mathcal{M}), the manifold \mathcal{H} becomes “attractive” again, and the system trajectory moves back to \mathcal{H} and then to \mathcal{M} . Therefore, as shown in Fig. 7, the system orbits gradually

Fig. 9. Enlarged time series around a burst in z_1 .Fig. 10. Time series of z_1 , $x_1 - x_2$, $y_1 - y_2$, Γ_1 , and d .

move towards the dashed lines (that is, \mathcal{M}) and finally get sufficiently close to \mathcal{M} once again, with another burst coming. In this way, intermittent blow-outs occur repeatedly. In other words, $z_i \approx z_*$, $i = 1, 2$, are quasi-synchronized in the long laminar phases, while they are desynchronized in the short burst phases.

Now, fix the parameters given in (9) and (10), where $\gamma = 0.34 > \gamma_c$. Fig. 9 shows the details near a burst of z_1 over time t . Moreover, Fig. 10 records the changes of z_1 , $x_1 - x_2$, $y_1 - y_2$, Γ_1 , and d over time t . Each time after the system orbit enters the laminar phase, d and $|\Gamma_i|$, $i = 1, 2$, begin to decrease, and, finally, the system orbit moves to \mathcal{M} so close that the system enters the burst phase. Thus, the intermittency can be characterized as follows: the laminar phase with $z_i \approx z_*$ is established repeatedly, and then it is broken when $|x_1 - x_2|$ and $|y_1 - y_2|$ almost vanish. Therefore, the irregular laminar lengths are, in fact, depending directly on the irregular burst magnitudes of $|\Gamma_i|$, $i = 1, 2$ (or, similarly, those of $|x_1 - x_2|$ and $|y_1 - y_2|$) at the bursting moments, denoted by $|\Gamma_i|_{\text{burst}}$, $i = 1, 2$ (or, correspondingly, $|x_1 - x_2|_{\text{burst}}$ and $|y_1 - y_2|_{\text{burst}}$). We can also see a clear relationship between the burst magnitudes and laminar lengths in the power law analysis to be given in the next section.

In \mathcal{H} , there are two limit cycles \mathcal{A} and \mathcal{M} . As discussed in the last subsection, limit cycle \mathcal{A} is a global attractor of system (1) if

Fig. 11. Time series of z_i , $i = 1, 2$, when $\gamma = 0.7$.

$\gamma < \frac{b}{a}$. However, when $\gamma > \frac{b}{a}$, \mathcal{A} is still stable in the \mathcal{H}^\perp direction (because the large coupling terms force the system orbits to approach \mathcal{H}), but it is unstable in the \mathcal{H} -direction (because $d \rightarrow 0$, instead of $d \rightarrow d^{\text{max}}$). However, \mathcal{M} is different. It is attractive in the \mathcal{H} -direction (since $d \rightarrow 0$), but it is unstable in the \mathcal{H}^\perp -direction (that is, it is transversely unstable). In fact, the intersection of the whole intermittent attractor of the discontinuous system (1) with \mathcal{H} is not equal to a (minimal) chaotic attractor in \mathcal{H} . Instead, it contains a limit cycle \mathcal{M} , which is transversely unstable, and another set \mathcal{A} , which is transversely stable. This matches the definition of in–out intermittency given by [1], [2], and [25], and we believe that the generated intermittency here also falls into the category of in–out intermittency, a generalized form of on–off intermittency, though the analysis of in–out intermittency has been given for smooth systems and the intermittency characteristics of smooth systems may somehow be different from those generated by discontinuous systems.

Of course, if the system parameters are changed significantly, the above analysis in this section may no longer be valid. For example, still with selecting parameter (9) but $\gamma = 0.7$ (which is much different from $\gamma_c = 0.3333$), the dynamical behavior shown in Fig. 11 is completely different from the intermittency when $\gamma = 0.34$ (quite close to γ_c) shown in Fig. 10.

Before the end of this section, we give a brief discussion about the influence of noise on the intermittency of system (1). Sometimes, intermittency may be sensitive to noise, and the noise energy, even if very small, may change significantly the transverse stability of an intermittent system, which may spoil the occurrence of intermittency. Here, an intermittency is said to be robust if the occurrence of this intermittency is not easily destroyed by noise. For example, the work reported in [12] shows that intermittent patterns almost vanish even if the noise magnitude is as low as 0.2% of the maximum magnitude of some corresponding system variables, which therefore is considered not robust. However, the numerical results shown in Fig. 12 demonstrate that the intermittent behavior here can be quite robust. Take two equations (the first equation on \dot{x}_1 and the third equation on \dot{z}_1) as an example (noticing that the two subsystems are identical and y_1 and x_1 are symmetric). As in [12], noise $w(t)$ is added to the right-hand side of the first equation (that is, the

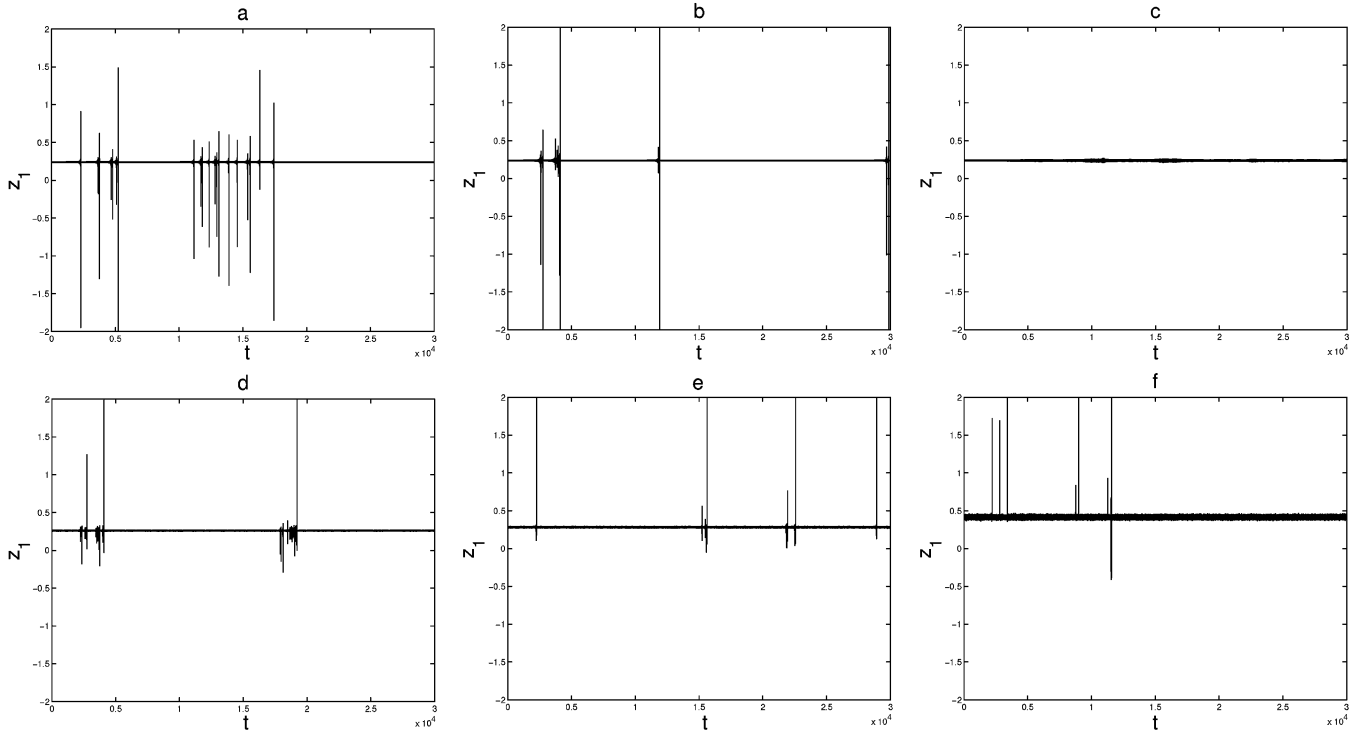


Fig. 12. Intermittency of z_1 in the following cases: (a) 5% noise added on the right-hand side of the first equation, (b) 10% noise added on the right-hand side of the first equation, (c) 20% noise added on the right-hand side of the first equation, (d) 5% noise added on the right-hand side of the third equation, (e) 10% noise added on the right-hand side of the third equation, and (f) 40% noise added on the right-hand side of the third equation.

equation on \dot{x}_1) with numerical results shown in Fig. 12(a)–(c), and the third equation (that is, the equation on \dot{z}_1), with numerical results shown in Fig. 12(d)–(f). The noise $w(t)$ is a uniform random signal with maximum magnitude being 5% [Fig. 12(a) and (d)], 10% [Fig. 12(b) and (e)], 20% [Fig. 12(c)], or 40% [Fig. 12(f)] of the maximum magnitude of x_1 or z_1 . When we added noise with 5% and 10% of the maximum magnitude of x_1 (or z_1) in equation \dot{x}_1 (or \dot{z}_1), respectively, the on–off intermittent patterns of z_1 remain prominent. Once the noise levels approximately become 20% in equation \dot{x}_1 and 40% in equation \dot{z}_1 , respectively, the intermittent patterns begin to vanish. Thus, one can see that the occurrence of the intermittency of the discontinuous system (1) is not very sensitive to noise.

IV. POWER LAW ANALYSIS

In spite of their irregular bursts, many intermittency phenomena display regularities including power laws. Such laws are used widely to describe natural complex phenomena. There are some well-known power laws for on–off/in–out intermittency, which have been considered before.

- I) The mean laminar length depends on the deviation of the control parameter from its critical value according to a power law with exponent -1 [13], [21].
- II) In the range of moderate lengths, the distribution of laminar lengths follows a power law with exponent $-\frac{3}{2}$, though in the range of large laminar lengths, the distribution exhibits an exponential decay [2], [13], [21].

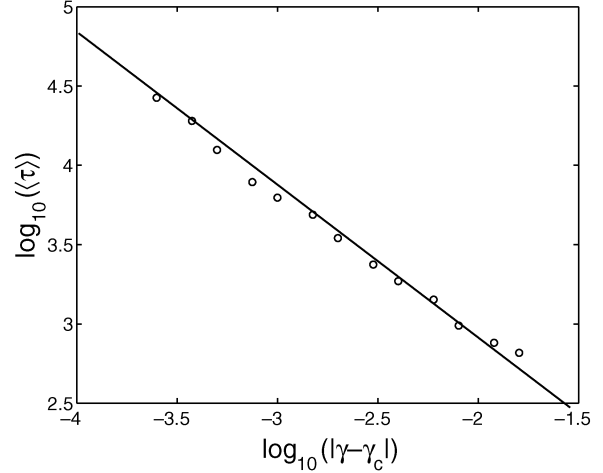


Fig. 13. Relation between $\langle \tau \rangle$ and $\gamma - (b/a)$.

- III) The burst amplitude satisfies -1 power law when its value is small (but the amplitude deviates from the power law when its value is large) [27].

In this section, we show that the intermittent phenomenon of the discontinuous system (1) also shares some power laws. For convenience, we denote by τ the length of the laminar phase. Then, we can show the relationship between its mean (that is, $\langle \tau \rangle$) and $\gamma - \frac{b}{a}$ when γ is slightly larger than b/a to maintain the intermittent phenomenon. Fig. 13 shows the change of the mean laminar length $\langle \tau \rangle$ over $\tilde{\gamma} = \gamma - \gamma_c > 0$ (with $\gamma_c = \frac{b}{a}$), which indicates clearly a power law

$$\langle \tau \rangle \propto \tilde{\gamma}^\alpha.$$

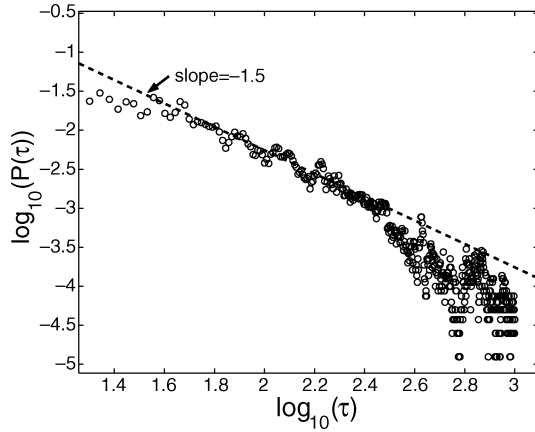


Fig. 14. Distribution of the laminar lengths.

Since $\alpha = -1.032 \approx -1$, this relation confirms the power law I) for the intermittency. From this, we can again verify the critical value $\gamma_c = \frac{b}{a}$.

Next, we investigate another statistical property; namely, the distribution of the laminar durations. Numerical analysis shows that the distribution of τ also follows a power law

$$P(\tau) \propto \tau^\beta$$

where the exponent is calculated as $\beta = 1.46$ when the range of τ is not large, verifying the power law II). In Fig. 14, the slope of the dashed line is -1.5 . Meanwhile, consistent with II), numerical results also suggest that the distribution tends to be exponential in the range of large τ .

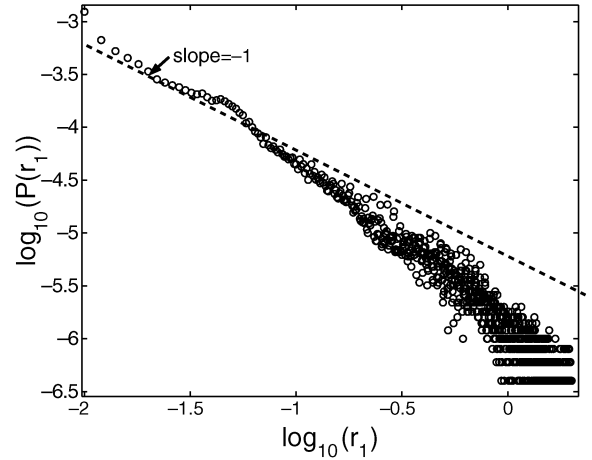
Then, let us check the burst amplitude of z_i , $i = 1, 2$, away from its mean laminar value z_* . For convenience, we only check z_1 and denote $r_1 = |z_1 - z_*|$. With parameters chosen as in (9) and (10), Fig. 15 presents a power law distribution of r_1 for z_1 (and the result for z_2 is similar) given as

$$P(r_1) \propto r_1^\lambda$$

when $r_1 = |z_1 - z_*|$ is small. Numerically, the exponent of the power law in a small range of r_1 is $\lambda = -1.069$, which is close to -1 (noting that the slope of the dashed line in Fig. 15 is -1). Therefore, $P(r_1)$ is consistent with the power law III), which was discussed for on-off intermittency in [27], though our intermittency is not a conventional on-off intermittency.

As stated in the last section, there are direct relationships between the laminar lengths and the burst amplitudes of $|\Gamma_i|$, $i = 1, 2$, or d (and $|x_1 - x_2|$ or $|y_1 - y_2|$) (referring to Fig. 10). Here, we confirm this by numerical results from the viewpoint of power law. In fact, Fig. 16 shows that the data of $|\Gamma_1|_{\text{burst}}$ (that is, the burst magnitude of $|\Gamma_1|$) follow a power law with exponent -1.43 and the data of d_{burst} with exponent -1.58 . In other words, these power laws are still quite close to the power law II) for τ with exponent -1.5 .

Thus, the variables or terms are closely related to laminar durations in the discontinuous system (1), as analyzed in the last section (referring to Fig. 10), sharing a power law with almost the same exponent -1.5 . In other words, the burst amplitudes

Fig. 15. Distribution of r_1 .

of these variables or terms in the intermittency follow the power law with exponent -1.5 , just like the power law II).

V. CONCLUSION AND REMARKS

Intermittency has drawn increasing attention in recent years, from many research communities, including physical sciences, biological sciences, and engineering. Many results on intermittency have been obtained but mostly for smooth systems (or continuous nonsmooth systems), which depend heavily on numerical simulations due to the very complex dynamical behaviors. Very few explicit expressions were given to characterize the intermittency in discontinuous systems. In this paper, we have investigated the intermittent phenomenon generated by a discontinuous system, composing of two simple switched subsystems coupled with a high strength, and studied the related intermittency mechanism. Our analysis of this discontinuous system has provided a better understanding of how intermittency occurs in nonsmooth systems.

Through the study in this paper, we conclude the following.

- 1) A new “in-out” intermittency can be generated by the simple discontinuous system (1), and the lower dimensional manifold \mathcal{H} for the intermittency results from the discontinuous switching mechanism.
- 2) There exist two limit cycles, which are transversely stable and unstable, respectively, in \mathcal{H} , and the intermittent bursts occur just before the two subsystems are almost completely synchronized (or, in other words, the “exiting” set in \mathcal{H} is the set of complete synchronization of all the state variables).
- 3) In the analysis of system (1), a simple approach is used, which is effective mainly because system (1) is simply constructed by switching between two almost “linear” systems.
- 4) The critical value of γ is closely related to system parameters, which is estimated as b/a . The intermittent phenomena can be generated when $\gamma > \frac{b}{a}$, and a nearly periodic motion can be observed when $\gamma < \frac{b}{a}$. In this sense, one can change a or b to control the occurrence of the intermittency.

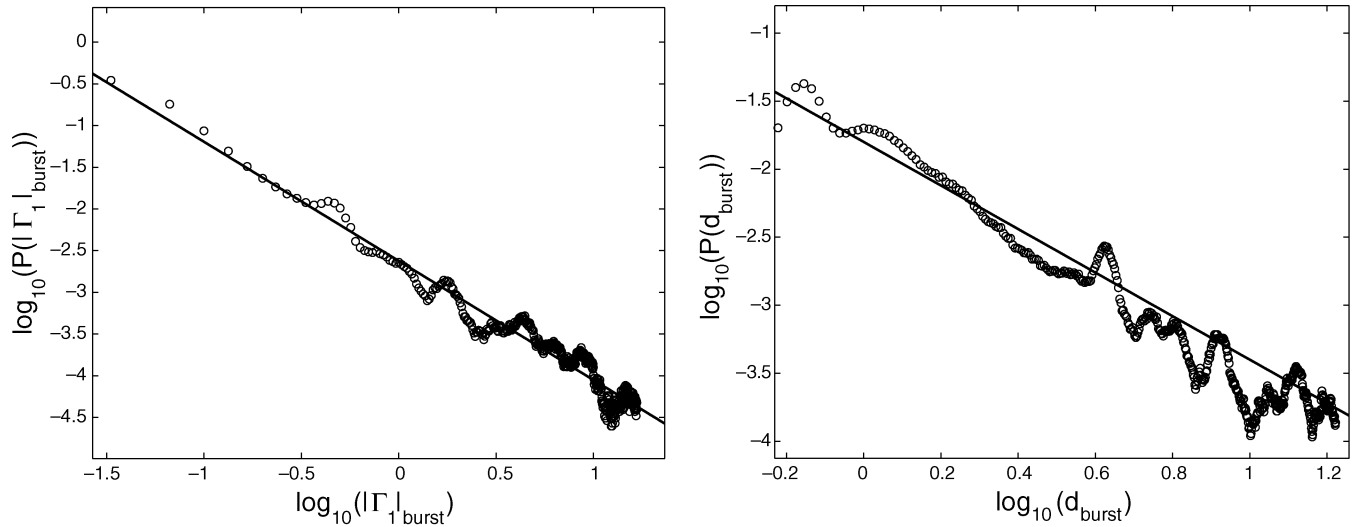


Fig. 16. Amplitude distribution of $|\Gamma_1|$ and d in the burst phase.

- 5) The mean values of z_i and R_i , $i = 1, 2$, in the laminar phase can be easily adjusted by controlling some parameters according to (24) or (25).
- 6) Power laws can be found in statistical studies of intermittent trajectories, and some other power laws have also been confirmed.

More detailed theoretical analysis and practical applications related to intermitencies produced by simple discontinuous systems, as well as efficient circuit implementation of various intermitencies, will be further investigated in future studies.

ACKNOWLEDGMENT

The authors wish to thank the anonymous reviewers for their constructive comments.

REFERENCES

- [1] P. Ashwin, E. Covas, and R. Tavakol, "Transverse instability for non-normal parameters," *Nonlinearity*, vol. 12, pp. 563–577, 1999.
- [2] —, "Influence of noise on scalings for in-out intermittency," *Phys. Rev. E*, vol. 64, p. 204, 2001.
- [3] M. S. Baptista and I. L. Calda, "Type-2 intermittency in the driven double scroll circuit," *Phys. D*, vol. 132, pp. 325–338, 1999.
- [4] J. M. Brooke, "Breaking of equatorial symmetry in a rotating system: a spiralling intermittency mechanism," *Europhys. Lett.*, vol. 37, no. 3, pp. 171–176, 1997.
- [5] J. Cabrera and J. Milton, "On-off intermittency in a human balancing task," *Phys. Rev. Lett.*, vol. 89, pp. 1587–1590, 2002.
- [6] A. Čenys, A. Namajūnas, A. Tamaševičius, and T. Schneider, "On-off intermittency in chaotic synchronization experiment," *Phys. Lett. A*, vol. 213, pp. 259–264, 1996.
- [7] G. Chen and X. Yu, *Chaos Control: Theory and Applications*. Berlin, Germany: Springer-Verlag, 2003.
- [8] Q. Chen, Y. Hong, G. Chen, and Q. Zhong, "Chaotic attractors in striped rectangular shapes generated by a Rössler-like system," *Phys. Lett. A*, vol. 348, pp. 195–200, 2006.
- [9] Q. Chen, Y. Hong, and G. Chen, "Chaotic behaviors and toroidal/spherical attractors generated by discontinuous dynamics," *Phys. A*, vol. 371, no. 2, pp. 293–302, Nov. 2006.
- [10] L. O. Chua and G. Lin, "Intermittency in a piecewise linear circuit," *IEEE Trans. Circuits Syst.*, vol. 38, no. 5, pp. 510–520, May 1991.
- [11] A. Filippov, *Differential Equations With Discontinuous Right Hand Side*. Dordrecht, The Netherlands: Kluwer, 1988.

- [12] A. Hasegawa, M. Komuro, T. Endo, and R. Igarashi, "A new type of intermittency from a ring of four coupled phase-locked loops," *IEEE Trans. Circuits Syst. I, Fundam. Theory Appl.*, vol. 45, no. 6, pp. 623–633, Jun. 1998.
- [13] J. F. Heagy, N. Platt, and S. M. Hammel, "Characterization of on-off intermittency," *Phys. Rev. E*, vol. 49, no. 2, pp. 1140–1150, 1994.
- [14] C. Kim, G. Yim, Y. Kim, J. Kim, and H. Lee, "Experimental evidence of characteristic relations of type-I intermittency in an electronic circuit," *Phys. Rev. E*, vol. 56, no. 3, pp. 2577–2593, 1997.
- [15] M. Kunze, *Non-Smooth Dynamical Systems*. Berlin, Germany: Springer-Verlag, 2000.
- [16] T. Kwok and K. Smith, "Optimization via intermittency with a self-organizing neural network," *Neural Comput.*, vol. 17, no. 11, pp. 2454–2481, 2005.
- [17] J. Lü and G. Chen, "Generating chaotic attractors with multiple merged basins of attraction," *IEEE Trans. Circuits Syst. I, Fundam. Theory Appl.*, vol. 50, no. 2, pp. 198–207, Feb. 2003.
- [18] J. Milton, J. Foss, J. Hunter, and J. Cabrera, "Controlling neurological disease at the edge of instability," in *Quantitative Neurosciences*, P. Pardalos, J. Sackellares, P. Carney, and L. Iasemidis, Eds. Boston, MA: Kluwer, 2004, pp. 117–143.
- [19] Y. Nagai, X.-D. Hua, and Y.-C. Lai, "Control of on-off intermittent dynamics," *Phys. Rev. E*, vol. 54, no. 2, pp. 1190–1199, 1996.
- [20] E. Ott, *Chaos in Dynamical Systems*. Cambridge, U.K.: Cambridge Univ. Press, 2002.
- [21] A. Pikovsky, "A new type of intermittent transition to chaos," *J. Phys. A*, vol. 16, pp. L109–L112, 1984.
- [22] N. Platt, E. A. Spiegel, and C. Tresser, "On-off intermittency: A mechanism for bursting," *Phys. Rev. Lett.*, vol. 70, pp. 279–282, 1993.
- [23] Y. Pomeau and P. Manneville, "Intermittent transition to turbulence in dissipative dynamical systems," *Commun. Math. Phys.*, vol. 74, pp. 189–197, 1980.
- [24] A. Slifkin, D. Vaillancourt, and K. Newell, "Intermittency in the control of continuous force production," *Neurophysiology*, vol. 7, pp. 298–312, 2000.
- [25] R. Sturman and P. Ashwin, "Internal dynamics of intermittency," in *Dynamics and Bifurcation of Patterns in Dissipative Systems*, ser. World Scientific Series on Nonlinear Science, G. Dangelmayr and I. Oprea, Eds. Singapore: World Scientific, 2004.
- [26] J. Suykens and J. Vandewalle, "Generation of n -double scrolls ($n = 1, 2, 3, 4, \dots$)," *IEEE Trans. Circuits Syst. I, Fundam. Theory Appl.*, vol. 40, no. 7, pp. 861–867, Jul. 1993.
- [27] C. Toniolo, A. Provenzale, and E. A. Spiegel, "Signature of on-off intermittency in measured signals," *Phys. Rev. E*, vol. 66, no. 6, p. 209, 2002.
- [28] V. Utkin, *Sliding Modes in Control Optimization*. Berlin, Germany: Springer-Verlag, 1992.
- [29] Y. Zhang and Y. Yao, "Controlling global stochasticity in the standard map," *Phys. Rev. E*, vol. 61, pp. 7219–7222, 2000.



Qingfei Chen received the B.E. and M.E. degrees from the Department of Automatic Control, Beijing Institute of Technology, Beijing, China, in 2003 and 2006, respectively. He is currently working toward the Ph.D. degree at the Department of Electrical Engineering, Arizona State University, Tempe.

His research interests include nonlinear dynamics, multi-agent systems, and complex networks.



Yiguang Hong (M'99–SM'02) received the B.Sc. and M.Sc. degrees from the Department of Mechanics, Peking University, Beijing, China, and the Ph.D. degree from the Chinese Academy of Sciences (CAS), Beijing, China.

He is currently a Professor with the Institute of Systems Science, Academy of Mathematics and Systems Science, CAS. His research interests include nonlinear dynamics and control, robot control, multi-agent systems, and reliability of software systems.

Dr. Hong was a recipient of the Guangzhaozhi Award of Chinese Control Conference in 1997, the Young Author Prize of the IFAC World Congress in 1999, the Young Scientist Award of CAS in 2001, and the Youth Award for Science and Technology of China in 2006.



Guanrong Chen (M'87–SM'92–F'97) received the M.Sc. degree in computer science from the Sun Yat-sen (Zhongshan) University, Guanzhou, China, and the Ph.D. degree in applied mathematics from Texas A&M University, College Station.

Currently, he is a Chair Professor and the Founding Director of the Centre for Chaos and Complex Networks, City University of Hong Kong.

Prof. Chen served and is serving as Chief Editor, Deputy Chief Editor, Advisory Editor, and Associate Editors for several international journals, including

the IEEE TRANSACTIONS ON CIRCUITS AND SYSTEMS (I AND II), the IEEE TRANSACTIONS ON AUTOMATIC CONTROL, and the *International Journal of Bifurcation and Chaos*. He was the recipient of the 1998 Harden–Simons Prize for the Outstanding Journal Paper Award from the American Society of Engineering Education, the 2001 M. Barry Carlton Best Annual Transactions Paper Award from the IEEE Aerospace and Electronic Systems Society, the 2002 Best Paper Award from the Institute of Information Theory and Automation, Academy of Science of the Czech Republic, and the 2005 IEEE Guillemin—Cauer Best Transaction Annual Paper Award from the Circuits and Systems Society. He is an honorary professor under different titles at several universities in Australia, China, and the United States.



David J. Hill (M'76–SM'91–F'93) received the B.E. and B.Sc. degrees from the University of Queensland, Brisbane, Australia, in 1972 and 1974, respectively, and the Ph.D. degree in electrical engineering from the University of Newcastle, Callaghan, Australia, in 1976.

He is currently an Australian Research Council Federation Fellow with the Research School of Information Sciences and Engineering, The Australian National University, Canberra. He has held academic and substantial visiting positions at the University of

Melbourne, University of California, Berkeley, University of Newcastle, Lund University, University of Sydney, and the City University of Hong Kong. He holds honorary professorships at the University of Sydney, Huazhong University of Science and Technology, the South China University of Technology, and the City University of Hong Kong. His research interests are in network systems, circuits and control with particular experience in stability analysis, nonlinear control and applications mainly to energy and information systems.

Dr. Hill is a Fellow of the Institution of Engineers, Australia, and a Foreign Member of the Royal Swedish Academy of Engineering Sciences.